



Human Kelch-like ECH-Associated Protein 1 (KEAP1)



A Target Enabling Package (TEP)

Gene ID / UniProt ID / EC	9817 / Q14145
Target Nominator	CHDI Foundation
SGC Authors	Roslin Adamson, Zhuoyao Chen, Sergio G. Bartual, Ritika Sethi, Peter Canning, Fiona J. Sorrell, Tobias Krojer, Frank von Delft, Alex N. Bullock
Collaborating Authors	Leticia Toledo-Sherman ¹
Target PI	Alex N. Bullock (SGC Oxford)
Therapeutic Area(s)	Neuropsychiatry
Disease Relevance	Inhibition of KEAP1 is thought to be cytoprotective for degenerative diseases such as Huntington's disease and multiple sclerosis by activating NRF2-dependent transcription of anti-oxidant genes.
Date Approved by TEP Evaluation Group	June 10, 2019
Document version	Version 1
Document version date	June 2019
Citation	Roslin Adamson, Zhuoyao Chen, Sergio G. Bartual, Ritika Sethi, Peter Canning, Fiona J. Sorrell, ... Alex N. Bullock. (2019). Human Kelch-like ECH Associated Protein 1 (KEAP1); A Target Enabling Package (Version 0) [Data set]. Zenodo. 10.5281/zenodo.3245339
Affiliations	¹ CHDI Management/CHDI Foundation, Los Angeles, CA, USA

USEFUL LINKS



Open Targets



ChEMBL



(Please note that the inclusion of links to external sites should not be taken as an endorsement of that site by the SGC in any way)

SUMMARY OF PROJECT

KEAP1 is a highly redox-sensitive member of the BTB-Kelch family that assembles with the CUL3 protein to form a Cullin-RING E3 ligase complex for the degradation of NRF2. Oxidative stress disables KEAP1 allowing NRF2 protein levels to accumulate for the transactivation of critical stress response genes. Consequently, the KEAP1-NRF2 system is a highly attractive target for the development of protein-protein interaction inhibitors that will stabilise NRF2 for therapeutic effect in conditions of neurodegeneration and inflammation. As part of this TEP we have solved the first crystal structure of a KEAP1-CUL3 complex as well as a structure of the apo-Kelch domain suitable for small molecule soaking. We further established a selectivity assay panel of 17 human Kelch domain-containing proteins and have shown that non-covalent KEAP1 inhibitors from the literature are highly selective for KEAP1. This protein panel offers a resource for future work on KEAP1 as well as 16 other human Kelch proteins.

SCIENTIFIC BACKGROUND

E3 ubiquitin ligases that direct substrate proteins to the ubiquitin proteasome system for degradation are promising, though still largely unexplored, drug targets. The multi-subunit Cullin-RING ligases (CRLs) represent the largest subclass of E3 ligase. CRLs are constructed around a Cullin-family protein (CUL1-5 or CUL7) that supports the binding of a substrate recruitment adaptor and a RING-domain containing protein (RBX1-2) for recruitment of E2-ubiquitin (1). Neddylation of the Cullin C-terminal domain enhances the association of the substrate and E2-ubiquitin centres to allow for efficient substrate ubiquitination (2).

The CUL3-based CRLs recruit BTB-domain proteins as their substrate-specific adaptors. The largest group are the Kelch-like (KLHL) family of proteins. These proteins contain an N-terminal BTB domain for CUL3 binding and a C-terminal Kelch domain for substrate recruitment. An intervening BACK (BTB and C-terminal Kelch) domain forms a helical linker between these domains and contains a 3-box motif that supports the high affinity BTB-CUL3 interaction (3). The BTB domain is typically homodimeric and is therefore associated with two copies of CUL3.

The best known KLHL-family substrate adaptor is KEAP1 (Kelch-like ECH-associated protein 1, KLHL19). KEAP1 regulates the oxidative stress and detoxification responses by controlling the levels of the transcription factor NRF2 (nuclear factor erythroid 2-related factor 2). Under normal conditions KEAP1 targets NRF2 for K48-linked polyubiquitination and proteasomal degradation (4,5). A single NRF2 molecule is thought to engage the two Kelch domains in the KEAP1 dimer by the presence of two separate degron motifs (the ETGE and DLG sites in NRF2). Crystal structures for these individual degrons bound to the KEAP1 Kelch domain have been solved previously (6,7). Upon cellular stress, cysteine covalent modification or oxidation in KEAP1 is predicted to disrupt its proper folding allowing NRF2 stabilisation and the subsequent activation of cellular defence genes carrying an Antioxidant Response Element (ARE) in their promoter (8) (Fig. 1).

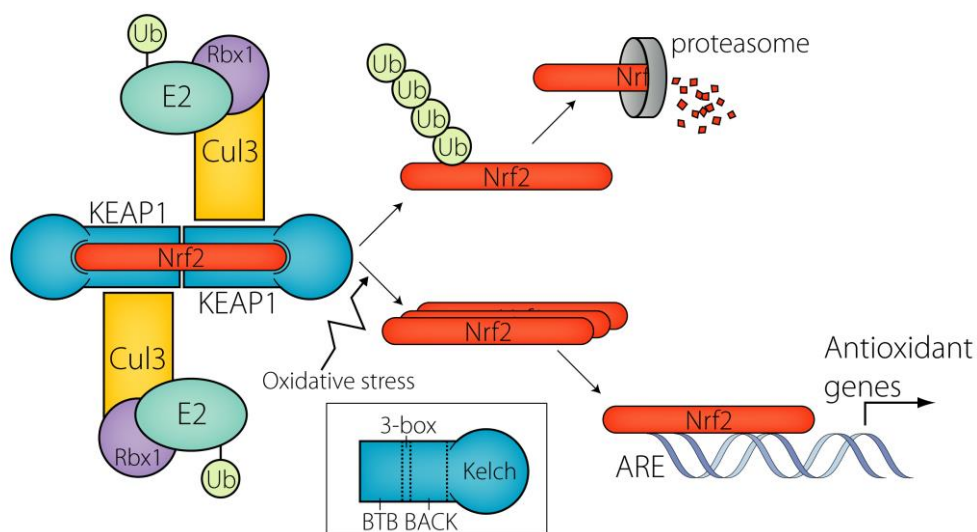


Fig. 1. KEAP1-dependent regulation of NRF2. Under basal conditions, NRF2 is polyubiquitinated by the KEAP1-CUL3 E3 ligase and subsequently degraded by the proteasome. Under conditions of oxidative stress the KEAP1 structure and function is disrupted and NRF2 ubiquitination is prevented. NRF2 accumulates and binds to antioxidant response elements (ARE) promoting transcription of over 200 cellular defence genes.

Loss of function mutations in KEAP1 are highly prevalent in lung cancer. The resulting activation of NRF2 in these tumour cells likely represents a survival adaptation to cellular stress caused by chemotherapy, radiotherapy or reactive oxygen species (9,10). Comparable inhibition of KEAP1 with small molecule inhibitors is considered an attractive therapeutic strategy for cytoprotection in a wide range of neurodegenerative diseases as well as chronic inflammatory, metabolic and respiratory diseases (10). This strategy is supported by further genetic association studies as protective SNPs that upregulate NRF2 pathways have been reported in amyotrophic lateral sclerosis, Alzheimer's disease and Parkinson's disease (10). Oxidative stress also appears

to be an important driver of Huntington disease and Friedreich's ataxia, and chemical inducers of NRF2 have shown beneficial responses in these disease models (10).

KEAP1 has been widely targeted by the pharmaceutical industry (10). Historically, most work has focussed on covalent inhibitors such as reactive electrophiles. One such compound, dimethyl fumarate (trade names, Fumaderm or Tecfidera), is an approved drug for remitting-relapsing multiple sclerosis. Another cysteine-reactive compound, bardoxolone methyl, is in phase 3 trials for diabetes patients with chronic kidney disease. Potential challenges with such treatments remain regarding target specificity, pharmacodynamics and safety (10). More recent work has begun to target the Kelch domain of KEAP1 with non-covalent compounds that may overcome some of these concerns. The most advanced non-covalent molecules have been developed by collaboration between GSK and Astex and include GSK-7 which has been crystallised with the Kelch domain for structure determination previously and exhibits a K_D of 1.3 nM (11,12).

In this TEP we have expanded the structural data for KEAP1 and developed a selectivity panel of human Kelch domain proteins to show that these non-covalent inhibitors are highly selective for KEAP1 over other family homologues.

RESULTS – THE TEP

Proteins purified

KEAP1 BTB-BACK-Kelch domains (used for assays)

Human KEAP1 BTB-BACK-Kelch domains (residues 48-624) were cloned into pFB-LIC-Bse for baculoviral protein expression in Sf9 cells. Protein was purified sequentially using Ni-affinity and size exclusion chromatography.

KEAP1 BTB-3-box domains (used for crystallography and assays)

Human KEAP1 BTB and 3-box domains (residues 48-213) were cloned into pNIC28-Bsa4, expressed in BL21(DE3)-R3-pRARE2 cells and purified sequentially using Ni-affinity and size exclusion chromatography.

Biotinylated KEAP1 BTB-3-box domains (used for assays)

Human KEAP1 BTB and 3-box domains (residues 48-213) were cloned into pNIC-Bio3, co-expressed in BL21(DE3)-R3-pRARE2 cells with BirA and biotin and purified sequentially using Ni-affinity and size exclusion chromatography.

KEAP1 Kelch domain (used for crystallography)

Human KEAP1 Kelch domain (residues 321-609) was cloned into pNIC28-Bsa4, expressed in BL21(DE3)-R3-pRARE2 cells and purified sequentially using Ni-affinity and size exclusion chromatography.

KEAP1 Kelch domain (used for assays)

Human KEAP1 Kelch domain (residues 321-624) was cloned into pNIC28-Bsa4, expressed in BL21(DE3)-R3-pRARE2 cells and purified sequentially using Ni-affinity and size exclusion chromatography.

CUL3NTD (used for crystallography and assays)

Human CUL3 N-terminal domain (NTD, residues 1-388, I342R/L346D mutant) was cloned into pNIC-CTHF, expressed in BL21(DE3)-R3-pRARE2 cells and purified sequentially using Ni-affinity and size exclusion chromatography.

KEAP1 BTB-3-box/CUL3NTD complex (used for crystallography)

Human KEAP1 BTB and 3-box domains (residues 48-213) and CUL3NTD (residues 1-388) proteins were expressed as above and purified separately by Ni-affinity chromatography. The proteins were mixed at 1:1 molar ratio and further purified by size exclusion chromatography.

Kelch selectivity panel proteins (used for crystallography and assays)

Human Kelch domains were expressed either in BL21(DE3)-R3-pRARE2 cells from a pNIC28-Bsa4 vector (KEAP1, KLHL2, KLHL3, KLHL7, KLHL11, KLHL12, KLHL17, KLHL20, KBTBD5, KBTBD10, KLHDC4), or utilising a pFB-LIC-Bse vector for baculoviral expression in Sf9 cultures (KLHL6, KLHL21, KBTBD7, KBTBD8, KLHDC5, KLHDC9). Proteins were purified using Ni-affinity and size exclusion chromatography. Full construct details are provided in the Materials and Methods section.

Structural data

KEAP1 structures

- 5NLB 3.45 Å structure of KEAP1 BTB-3-box in complex with CUL3NTD
- 6ROG 2.16 Å structure of apo-Kelch domain of KEAP1

Other BTB-Kelch family structures solved at SGC

- 2XN4 1.99 Å structure of apo-Kelch domain of KLHL2
- 4CHB 1.56 Å structure of the Kelch domain of KLHL2 in complex with WNK4 peptide
- 4CH9 1.84 Å structure of the Kelch domain of KLHL3 in complex with WNK4 peptide
- 5NKP 2.8 Å structure of the Kelch domain of KLHL3 in complex with WNK3 peptide
- 3II7 1.63 Å structure of the apo-Kelch domain of KLHL7
- 3I3N 2.6 Å structure of the BTB-BACK domains of KLHL11
- 4AP2 2.8 Å structure of the BTB-BACK domains of KLHL11 in complex with CUL3NTD
- 4APF 3.1 Å structure of the BTB-BACK domains of KLHL11 in complex with CUL3NTD Δ N22
- 2VPJ 1.85 Å structure of the apo-Kelch domain of KLHL12
- 6HRL 2.6 Å structure of the apo-Kelch domain of KLHL17
- 6GY5 1.09 Å structure of the Kelch domain of KLHL20 in complex with DAPK1 peptide
- 4ASC 1.78 Å structure of the apo-Kelch domain of KLHL40 (KBTBD5)

Overall architecture of the KEAP1-CUL3 E3 ligase

To confirm the overall dimeric architecture and CUL3 binding of KEAP1 we solved the structure of its BTB and 3-box domains in complex with the CUL3NTD (N-terminal domain) (**Fig. 2A**). We also separately solved the structure of the C-terminal Kelch domain (**Fig. 2A**). In previous work we had additionally solved the structure of the complete BTB-BACK domains of KLHL11 in complex with CUL3NTD (PDB [4AP2](#)) (3). Together these structures allow a model to be constructed for the full KEAP1 dimer (**Fig. 2B**). A flexible linker of approximately 20 residues is predicted between the BACK and Kelch domains. This linker may have hindered structural studies of the full length KEAP1 protein. It also creates uncertainty as to how the Kelch domain may position atop the BACK domain and how flexible this packing may be. Structural homology between different Cullin proteins also allows the structural model to be extended to a complete Cullin-RING ligase complex as published (**Fig. 2B**) (3,13). The model shows two E2-ubiquitin moieties poised over the substrate to achieve ubiquitination.

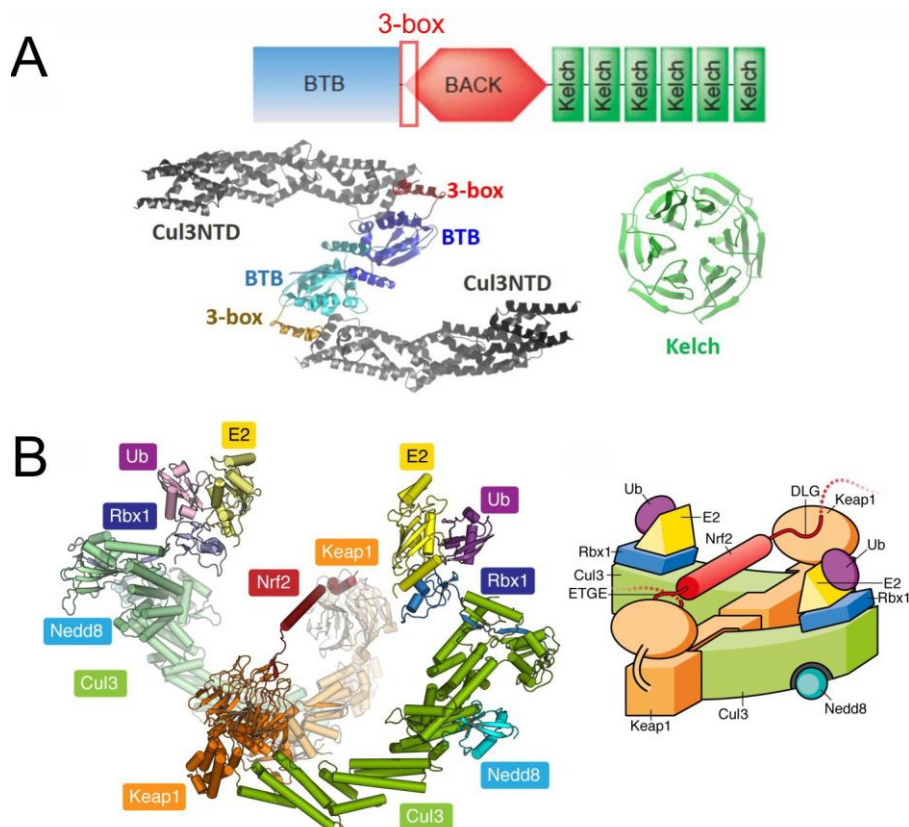


Fig. 2. Overall architecture of the KEAP1-CUL3 E3 ligase. **(A)** Domain organisation of KEAP1 and overview of the solved KEAP1 structures in this TEP. (Left) Dimeric KEAP1 BTB-3-box bound to CUL3NTD. (Right) Apo-Kelch domain. **(B)** Model of the fully assembled KEAP1 Cullin-RING ligase in complex with NRF2 substrate and E2-Ubiquitin.

Differences between the KEAP1 and KLHL11 complexes with CUL3

The more complete structure of KLHL11 (26.5 % sequence identity over the BTB-3-box) revealed previously that the 3-box folds as a two-helix motif that forms a hydrophobic groove between the BTB and BACK domains (**Fig. 3A**). The structure of a KLHL11-CUL3 complex further revealed that the CUL3NTD contains an N-terminal extension that occupies this groove to extend the binding interface (**Fig. 3B**). Deletion of the N-terminal 22 residue extension in CUL3 was found to reduce the CUL3 binding affinity of KLHL11 by 30-fold (3). Notably, this N-terminal CUL3 extension was not observed in the electron density maps for the KEAP1-CUL3 complex (**Fig. 2A**). This may reflect the absence of the remainder of the BACK domain in the crystallised construct, or sequence differences in the 3-box groove between KLHL11 and KEAP1. We also observed using BIAcore experiments that the binding of full length KEAP1 to CUL3 was considerably weaker than the equivalent KLHL11 interaction suggesting that the structural differences may be significant (see assay section below).

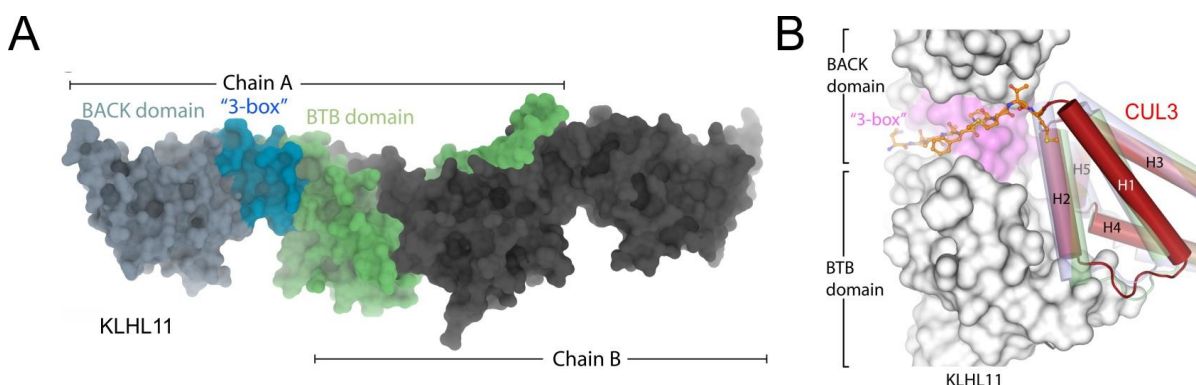


Fig. 3. Additional features in the KLHL11-CUL3 complex structure. **(A)** Structure of the complete KLHL11 BTB-BACK domains showing the 3-box as a hydrophobic groove. **(B)** The KLHL11-CUL3 structure revealed an N-terminal extension in CUL3 that bound to the 3-box groove. The same CUL3 extension was not observed in the KEAP1-CUL3 crystal structure discussed above.

Structure of the KEAP1 Kelch domain in a soakable crystal form

The solved structure of the KEAP1 Kelch domain revealed two protein chains in the asymmetric unit (**Fig. 4A**). Comparison with other ligand-bound KEAP1 structures indicated that the binding pocket was not obscured by crystal packing and that the apo-crystal form was suitable for soaking as experimentally validated.

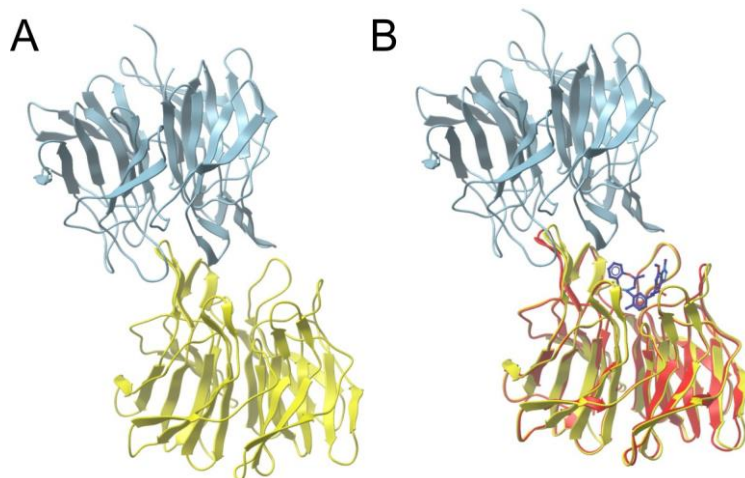


Fig. 4. Structure of the KEAP1 Kelch domain. **(A)** Two Kelch domains were observed in the asymmetric unit. **(B)** Superposition of a KEAP1 Kelch domain (red) in complex with the small molecule GSK-7 (dark blue sticks, 5FNU) shows that the apo-KEAP1 crystal form (yellow and cyan) is a soakable system in which the packing does not block the binding pocket.

Intra-family structural diversity in the Kelch substrate pocket

Comparison of the solved Kelch domain structures revealed that the substrate-binding pocket was divergent across the different BTB-Kelch family members. This was reflected in the alternative substrate binding poses in the substrate complexes of KEAP1, KLHL3 and KLHL20 (**Fig. 5A**). The low sequence conservation across the Kelch domains was also reflected in the variation observed in their electrostatic surface potential (**Fig. 5B**).

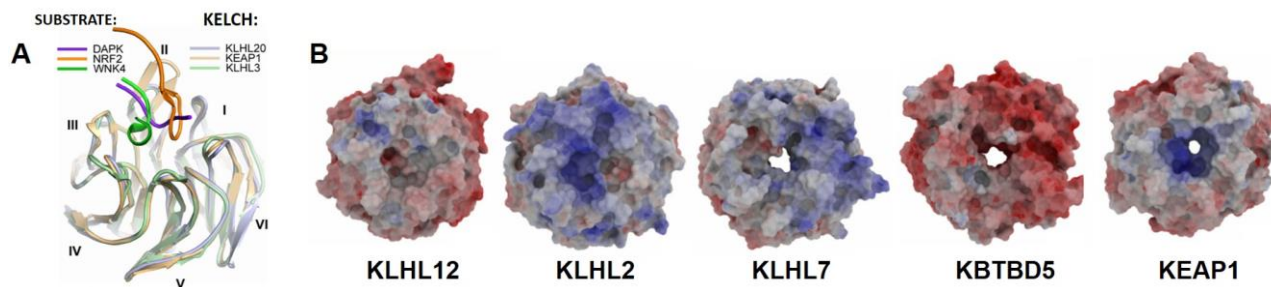


Fig. 5. Structural diversity across different Kelch domain substrate pockets. **(A)** Superposition of the KEAP1-NRF2, KLHL3-WNK4 and KLHL20-DAPK1 complex structures reveals alternative substrate peptide binding modes. **(B)** The substrate binding pockets across the BTB-Kelch family show different pocket shapes and electrostatic surface potential.

Assays

Biophysical characterisation of the KEAP1 interaction with CUL3

Bi-layer interferometry (BLI) was used to determine the affinity of the interaction between KEAP1 BTB-3-box and CUL3NTD. Biotinylated KEAP1 was immobilised on streptavidin-coated Octet sensors (ForteBio) buffered in 50 mM HEPES, 300 mM NaCl, 0.5 mM TCEP, 10 mM DTT. Binding was measured using serial dilutions of CUL3NTD in the same buffer plus 0.01 % Tween or buffer reference wells. A steady state fit for the binding indicated $K_D = 1.8 \mu\text{M}$ (**Fig. 6**). Similar results were obtained by SPR or by immobilising biotinylated CUL3NTD (data not shown). This dissociation constant is similar to that observed for the SPOP BTB domain binding to CUL3NTD ($K_D = 1.0 \mu\text{M}$) (14). However, it is significantly weaker than the binding of the full KLHL11 BTB-BACK domain construct binding to CUL3NTD ($K_D = 20 \text{ nM}$). These data suggest the

importance of the complete BACK domain. Unfortunately, a dimeric BTB-BACK-Kelch construct of KEAP1 showed poor behaviour during these binding experiments preventing measurements of its binding to CUL3NTD.

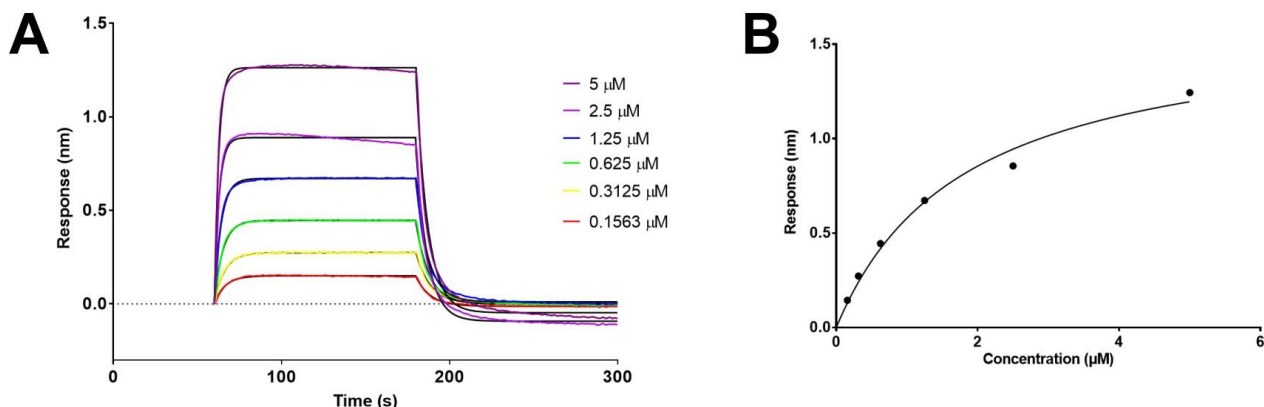


Fig. 6. Binding of CUL3NTD to KEAP1 BTB-3-box. (A) Double referenced curves showing CUL3NTD binding to KEAP1 BTB-3-box at increasing concentrations. Black lines show the fits to the experimental data. (B) Steady state analysis of the binding curves indicates $K_D = 1.8 \mu\text{M}$.

Selectivity panel for screening small molecule inhibitors of Kelch domain E3 ligases

We collaborated with the CHDI Foundation to characterize the binding potency and selectivity of 8 literature and proprietary non-covalent inhibitors of the KEAP1 Kelch domain (Fig. 7A).

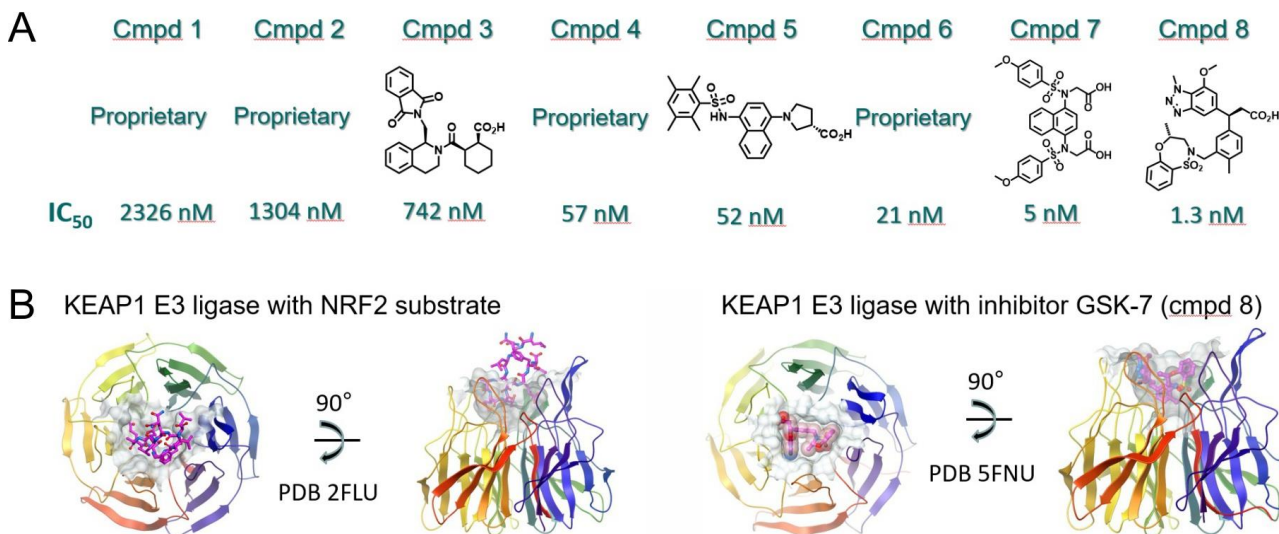


Fig. 7. KEAP1 Kelch domain inhibitor panel. (A) Panel of non-covalent inhibitors targeted to the Kelch domain of KEAP1. Compounds and their IC_{50} values were provided by the CHDI Foundation. (B) Exemplar ligand co-structures of the KEAP1 Kelch domain. Small molecule inhibitors compete with the substrate for binding.

Such molecules have been developed by several pharma to target the E3 substrate binding site (Fig. 7B). However, little data exist to assess whether these inhibitors possess the same high levels of selectivity as natural E3 substrates. One difficulty is that other BTB-Kelch E3 ligases are less well characterised such that peptide displacement assays for IC_{50} determination are not possible. We therefore explored whether differential scanning fluorimetry could be used as a thermal shift assay to measure compound binding potency. As shown in Fig. 8 there was an excellent correlation between the inhibitor $\text{Log } IC_{50}$ values and T_m shift values validating this as a generic assay format to cross-screen small molecule KEAP1 inhibitors against other human Kelch domains.

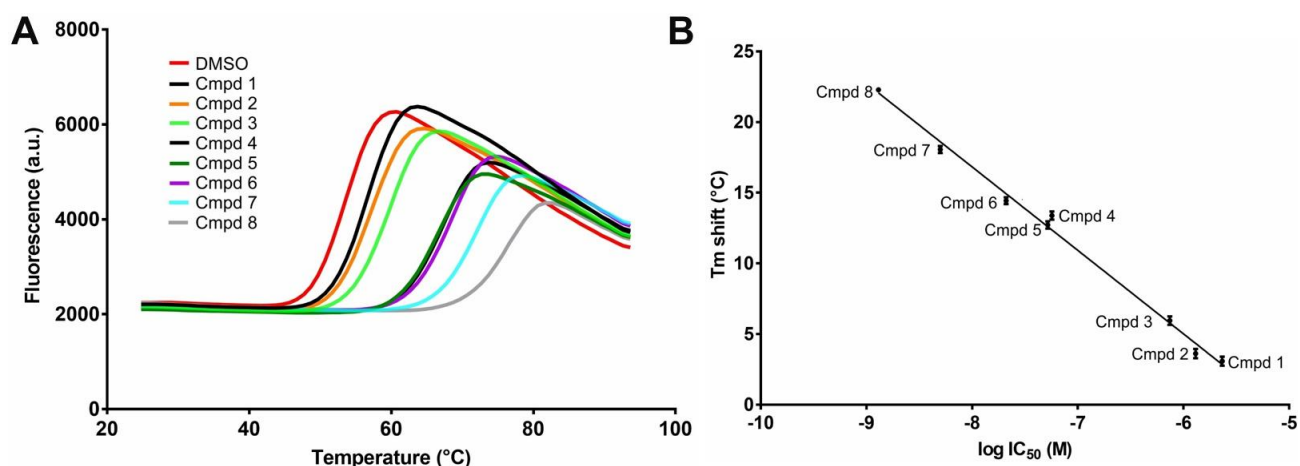


Fig. 8. Inhibitor IC_{50} values correlate with T_m shift values. **(A)** Thermal denaturation curves of KEAP1 Kelch domain in the presence of 2.5% DMSO or 12.5 μ M compound. **(B)** Plot to show the correlation between inhibitor Log IC_{50} values and T_m shift values.

Humans express over 50 Kelch domain proteins. We prepared a panel of 17 Kelch-containing proteins for screening (**Fig. 9A**). Most protein constructs contained the isolated Kelch domain. However, recombinant KLHL11 was only recovered when expressed as a construct also containing the BACK domain. The KLHDC family Kelch proteins are less characterised with regard to their folding outside the Kelch domain as variable construct boundaries were used that were optimised for recombinant expression. Interestingly, the panel of proteins exhibited a large range of protein melting temperatures (**Fig. 9B**)

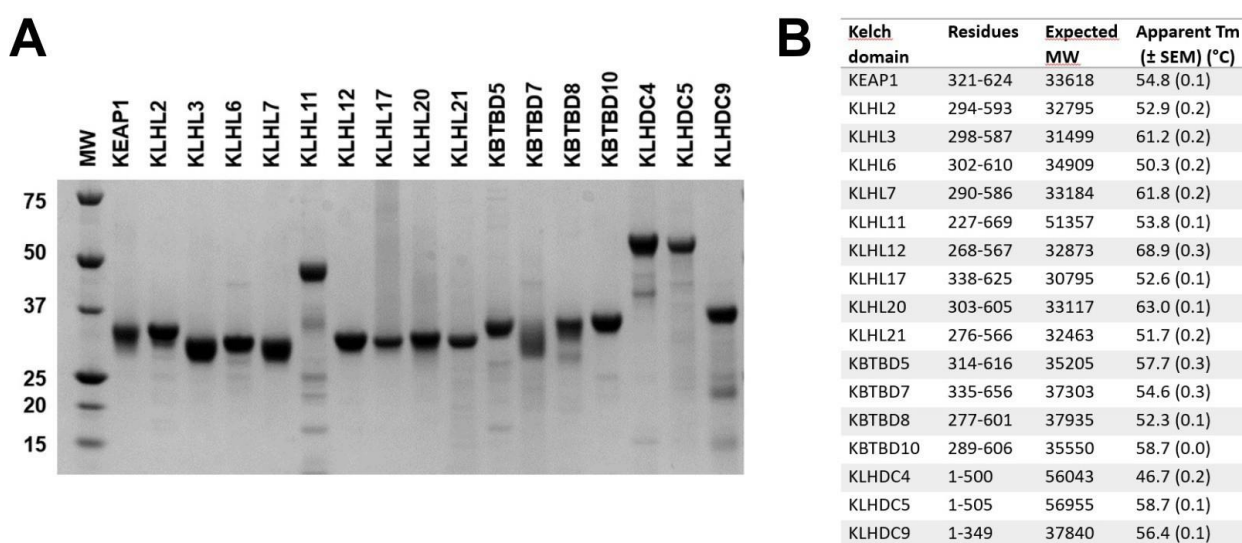


Fig. 9. Human Kelch domain protein panel. **(A)** SDS PAGE of purified recombinant proteins. **(B)** Construct details and apparent T_m (in absence of compound or DMSO).

The panel of 17 human Kelch proteins was then tested in the differential scanning fluorimetry assay in the presence of different small molecule KEAP1 inhibitors. As shown in **Fig. 10**, KEAP1 exhibited clear observable T_m shifts of up to 22.3 $^{\circ}$ C (compound 8, GSK-7). None of the other Kelch proteins showed a T_m shift above background. These data indicate the KEAP1 inhibitors in this panel are highly selective for KEAP1 over other Kelch domains. This likely reflects their diverse sequence, pocket dimensions and surface charge (**Fig. 5**).

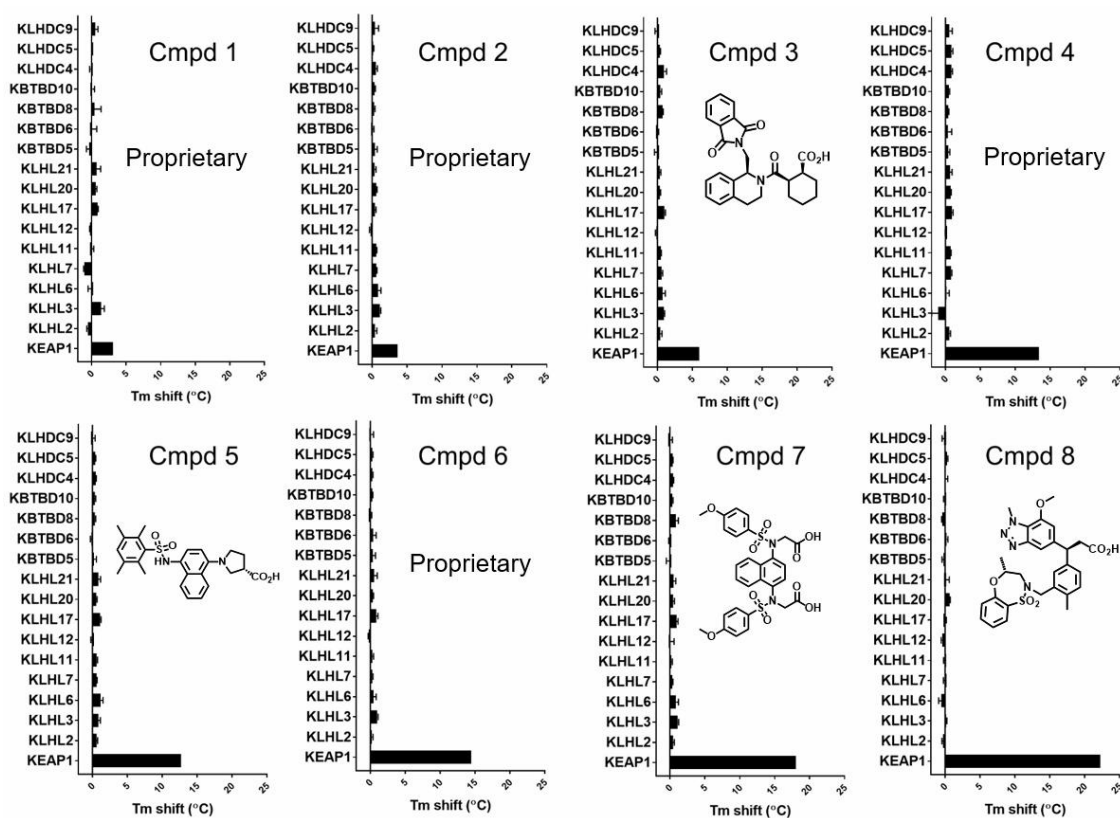


Fig. 10. Inhibitor selectivity profiles. T_m shift values are plotted for different Kelch proteins in the presence of indicated non-covalent KEAP1 inhibitors.

Chemical Matter

In this TEP, we collaborated with the CHDI Foundation to characterize the known literature compounds as well as some compounds proprietary to CHDI. This chemical matter is shown in **Fig. 7A**.

IMPORTANT: Please note that the small molecules within this TEP were generated by external sources. Structural and/or assay data indicate that they are likely to bind to the protein in potentially functionally relevant locations within the Kelch domain of KEAP1. Users may refer to the external literature for guidelines as to the potential use of such compounds in cellular studies.

Antibodies

Commercial antibodies against KEAP1 are available and validated in the literature, although they have not been tested at the SGC.

CRISPR/Cas9 reagents

CRISPR/Cas9 reagents for KEAP1 are described in the literature as well as commercial catalogues, although they have not been tested at the SGC.

Future plans

Further chemistry is planned to expand the repertoire of inhibitors to other BTB-Kelch family E3 ligases for which the selectivity panel assembled here will be most valuable. Further work to develop suitable assays for these targets is also underway.

Collaborations

CHDI Foundation: Leticia Toledo-Sherman

CONCLUSION

Genetic data and disease models suggest that KEAP1 inhibition may be a valuable cytoprotective approach for treatment of a wide range of neuropsychiatric and dementia conditions. Accordingly, a number of

different therapeutic strategies have been formulated, particularly targeting either reactive cysteines in KEAP1 or through non-covalent inhibitors of the Kelch domain (**Fig. 11**) (15).

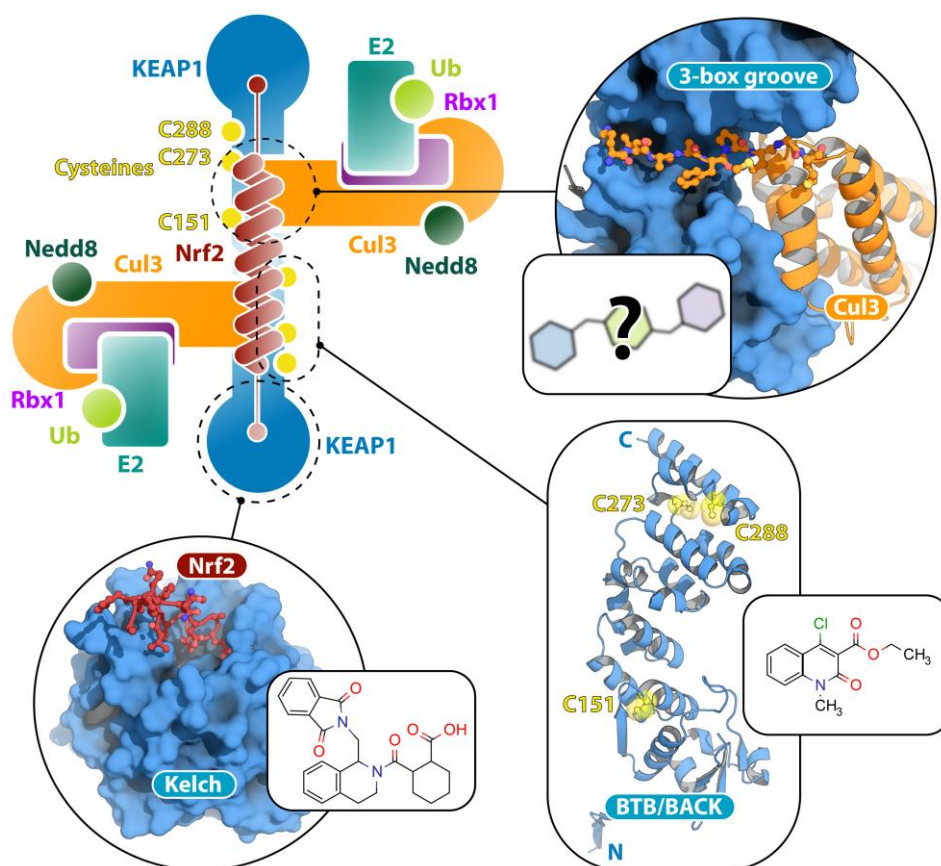


Fig. 11. Schematic of the full KEAP1 CRL3 complex structure with interfaces currently and potentially targeted by small molecule inhibitors. The KEAP1-NRF2 structure (PDB ID: 2FLU) (6) is shown with an example inhibitor of this interaction (16). The BTB-BACK structure is modelled from the structure of KLHL11 (PDB ID: 3I3N) (3) with cysteine residues modelled known to be covalently modified by the displayed small molecule (17). The surface representation of the 3-box groove is taken from the homologous structure of the KLHL11-CUL3 complex (PDB ID: 4AP2) (3). It is unclear if this groove is also targetable for inhibition of KEAP1. Figure taken from (15).

Covalent inhibitors of KEAP1 have concerns regarding target specificity, pharmacodynamics and safety (10). Here we show that non-covalent inhibitors of the Kelch domain achieve high selectivity across a panel of 17 human Kelch domain-containing proteins. As part of this TEP, we provide a set of structures and assays to support the continued development of these molecules. In addition, many of the reported recombinant Kelch proteins and structures may be new targets for compound screening, potentially allowing development of a wider repertoire of E3 ligase handles for PROTAC development.

TEP IMPACT

Manuscripts describing the structures and assays in this TEP are currently in preparation. Other review and primary papers associated with work in this TEP are published and listed below.

- Canning, P., et al., [Structural basis for Cul3 protein assembly with the BTB-Kelch family of E3 ubiquitin ligases](#). *J Biol Chem*, 2013. 288(11): p. 7803-14.
- Canning, P. and A.N. Bullock, [New strategies to inhibit KEAP1 and the Cul3-based E3 ubiquitin ligases](#). *Biochem Soc Trans*, 2014. 42(1): p. 103-7
- Schumacher, F.R., Sorrell, F.J., Alessi, D.R., Bullock, A.N., Kurz, T., [Structural and biochemical characterization of the KLHL3-WNK kinase interaction important in blood pressure regulation](#). *Biochem J*, 2014. 460(2): p. 237-46.

- Canning, P., F.J. Sorrell, and A.N. Bullock, [Structural basis of Keap1 interactions with Nrf2](#). *Free Radic Biol Med*, 2015. 88(Pt B): p. 101-107.
- Chen, Z., Picaud, S., Filippakopoulos, P., D'Angiolella, V., Bullock, A.N., [Structural basis for recruitment of DAPK1 to the KLHL20 E3 ligase](#). *bioRxiv*, 2018.

FUNDING INFORMATION

The work performed at the SGC has been funded by a grant from Wellcome [106169/ZZ14/Z]. Roslin Adamson and Sergio G. Bartual acknowledge additional support from the CHDI Foundation. Zhuoyao Chen acknowledges DPhil support from a China Scholarship Council-University of Oxford Scholarship. Ritika Sethi acknowledges additional support from the European Lead Factory.

ADDITIONAL INFORMATION

Structure Files

PDB ID	Structure Details
5NLB	3.45 Å structure of KEAP1 BTB-3-box in complex with CUL3NTD
6ROG	2.16 Å structure of apo-Kelch domain of KEAP1
2XN4	1.99 Å structure of apo-Kelch domain of KLHL2
4CHB	1.56 Å structure of the KLHL2 Kelch domain with WNK4 peptide
4CH9	1.84 Å structure of the KLHL3 Kelch domain with WNK4 peptide
5NKP	2.8 Å structure of the KLHL3 Kelch domain with WNK3 peptide
3II7	1.63 Å structure of the apo-Kelch domain of KLHL7
3I3N	2.6 Å structure of the BTB-BACK domains of KLHL11
4AP2	2.8 Å structure of the KLHL11 BTB-BACK domains with CUL3NTD
4APF	3.1 Å structure of the KLHL11 BTB-BACK with CUL3NTDΔN22
2VPJ	1.85 Å structure of the apo-Kelch domain of KLHL12
6HRL	2.6 Å structure of the apo-Kelch domain of KLHL17
6GY5	1.09 Å structure of the KLHL20 Kelch domain with DAPK1 peptide
4ASC	1.78 Å structure of the apo-Kelch domain of KLHL40 (KBTBD5)

Materials and Methods

Mass Spectrometry

Protein masses were determined using an Agilent LC/MSD TOF system with reversed-phase high-performance liquid chromatography coupled to electrospray ionization and an orthogonal time-of-flight mass analyser. Proteins were desalted prior to mass spectrometry by rapid elution off a C3 column with a gradient of 5-95% isopropanol in water with 0.1% formic acid. Spectra were analysed using the MassHunter software (Agilent).

Protein Expression and Purification

Human KEAP1 Kelch domain

Boundaries: residues 321-624

Expressed protein sequence:

MHHHHHHSSGVDLGTENLYFQSMAPKVGRLIYTAGGYFRQSLSYLEAYNPSDGTWLRRLADLQVPRSLAGCVVGGLLYAV
GGRNNSPDGNTDSSALDCYNPMTNQWSPCAPMSVPRNRIGVGVIDGHIYAVGGSHGCIHNSVERYEPERDEWHLVAP
MLTRRIGVGVAVLNRLLYAVGGFDGNTNRLNSAECYPERNEWRMITAMNTIRSGAGVCVLHNCIYAAGGYDGGDQLNSVE
RYDVETETWTFVAPMKHRRSALGITVHQGRIYVLLGGYDGHFTLDSVECYDPDPTDTWSEVTRMTSGRSGVGVAVTMEPCRK
QIDQQNCTC

Vector: pNIC28-Bsa4

Tag and additions: TEV-cleavable N-terminal hexahistidine tag

Expression cell: E. coli BL21(DE3)R3-pRARE2

The Kelch domain of human KEAP1 was expressed in *E. coli* (BL21(DE3)-R3-pRARE2) cells with a TEV-cleavable 6xHis tag. Cell cultures were grown in TB medium at 37 °C until the OD600 reached 0.8. Protein expression was induced with 1 mM IPTG for 16 h at 18 °C. Cells were spun at 5000 rpm for 10 min, then resuspended in binding buffer (20mM TRIS pH 7.5, 300 mM NaCl, 5 mM Imidazole) and frozen at -80°C. After thawing, the cells were lysed using an Emulsiflex C5 homogeniser by sonication. After centrifugation at 4 °C, the supernatant was applied to a His GraviTrap column (GE healthcare) equilibrated with binding buffer. After washing with binding buffer, KEAP1 was eluted with binding buffer supplemented to 500 mM imidazole. The eluted protein was applied to a PD-10 desalting column (GE Healthcare) and eluted with binding buffer. The N-terminal affinity tag was removed by TEV cleavage overnight and uncleaved protein was removed by applying it again to a His GraviTrap column. The flow-through was concentrated and purified further by size exclusion chromatography using a HiLoad 26/600 Superdex 75 pg (GE Healthcare Life Sciences) column equilibrated with gel filtration buffer (20mM TRIS pH 7.5, 300 mM NaCl, 1 mM TCEP). Fractions containing protein were pooled, concentrated to 12 mg/mL and stored at -80°C.

Human KEAP1 BTB-3-box and CUL3NTD complex

Boundaries: KEAP1 residues 48-213 and CUL3 residues 1-388

Expressed protein sequence (KEAP1):

MHHHHHSSGVDLGTENLYFQSMGNRTFSYTLLEDHTKQAFGIMNELRLSQQLCDVTLQVKYQDAPAAQFMAHKVVLASS
SPVFKAMFTNGLREQGMEVVSIEGIHPKVMERLIEFAYTASISMGEKCVLHVMNGAVMYQIDSVVRACSDFLVQQLDPSNA
IGIANFAEQIGCVLHQRAREYIYMHFGE

Expressed protein sequence (CUL3NTD):

MSNLSKGTGSRKDTKMIRAFPMTMDEKYVNSIWDLLKNAIQEIQRKNNSGLSFEELYRNAYTMVLHKKHGEKLYTGLREV
TEHLINKVREDVNLNLFQTLNQAANDHQTAMVMIRDILMYMDRVVYQNNVENVNGLIIFRDQVVRGICIRDH
LRQTLDMIARERKGEVVDRAIRNACQMLMILGLEGRSVYEEDEAPFLEMSAEFFQMSQKFLAENSASVYIKKVEARINE
EIERVMHCLDKSTEEPIVKVVERELISKHMKTIVEMENSGLVHMLKNGKTEDLGCMYKLSRVPNGLTKMCECMSSYLREQG
KALVSEEGEGKNPVDYRQGLDDLKSRFDRFLLESFNNDRLFKQTIAGDFEYFLNLSRSPEYLAENLYFQSHHHHHHDYKDD
DK

Vector: pNIC28-Bsa4 (KEAP1) and pNIC-CTHF (CUL3NTD)

Tag and additions: TEV-cleavable N-terminal hexahistidine tag (KEAP1); TEV-cleavable C-terminal hexahistidine and Flag tags (CUL3NTD)

Expression cell: E. coli BL21(DE3)R3-pRARE2

Human KEAP1 (Uniprot Q14145, residues 48-213 (BTB-3-box)) was subcloned into the vector pNIC28-Bsa4, and human CUL3NTD (Uniprot Q13618, residues 1-388, or where desired residues 23-388 (CUL3NTD Δ N22)), was subcloned into the vector pNIC-CTHF using ligation-independent cloning. Two point mutations (I342R and L346D) were introduced into the CUL3 sequence to stabilize the isolated N-terminal domain (NTD). Proteins were expressed separately overnight at 18°C in BL21(DE3)R3-pRARE2 cells in the presence of kanamycin and chloramphenicol, with 0.25 mM IPTG for induction. The harvested cells (2-3 L) were resuspended in 40 mL Binding Buffer (50 mM HEPES pH 7.5, 500 mM NaCl, 5 % glycerol, 5 mM imidazole and 0.5 mM TCEP) per 2 L cell culture. Lysozyme (1 mg/mL), PEI (1 mL of 5% stock) and protease inhibitors were added and the cells sonicated. After centrifugation of the lysate at 50 000 g the supernatant was filtered (1.2 μ m) and incubated with 3 mL Ni²⁺ sepharose resin equilibrated in Binding Buffer, for 30 min. The column was washed with 50-80 mL Wash Buffer (50 mM HEPES pH 7.5, 500 mM NaCl, 5 % glycerol, 30 mM imidazole and 0.5 mM TCEP) and the proteins eluted in 10 mL fractions with each of Elution buffers 1-4 (Binding Buffer with increasing concentrations of imidazole: 50, 100, 150 and 250 mM). The fractions were pooled, diluted one third with binding buffer and tobacco etch virus (TEV) protease added for overnight incubation to remove the hexahistidine tags. The samples were concentrated, KEAP1 and CUL3 mixed together in a 1:1 molar ratio and incubated for 2 hours on ice, before size exclusion purification on a 16/60 Superdex S200 column at 4°C in Gel Filtration (GF) Buffer (50 mM HEPES pH 7.5, 300 mM NaCl, 0.5 mM TCEP). Peak fractions were pooled, concentrated with 10 mM DTT and used in crystal trials.

Human KEAP1 BTB-BACK Kelch domains

Boundaries: residues 48-624

Expressed protein sequence:

MGHHHHHSSGVDLGTENLYFQSMGNRTFSYTLLEDHTKQAFGIMNELRLSQQLCDVTLQVKYQDAPAAQFMAHKVVLAS
SSPVFKAMFTNGLREQGMEVVSIEGIHPKVMERLIEFAYTASISMGEKCVLHVMNGAVMYQIDSVVRACSDFLVQQLDPSNA
AIGIANFAEQIGCVLHQRAREYIYMHFGEVAKQEENLNSHCQLVTLISRDDLNVRCSESEVFHACINWVKYDCEQRRFYVQA
LLRAVRCHSLTPNLFQMLQKCEILQSDSRCKDYLVKIFEELTLHKPTQVMPCRAPKVGRLIYTAGGYFRQSLSYLEAYNPSDG
TWLRLADLQVPRGLAGCVVGGLLYAVGGRRNSPDGNTDSSALDCYNPMTNQWSPCAPMSVPRNRIGVGVIDGHIYAVG
GSHGCIHHNSVERYEPERDEWHLVAPMLTRRIGVGVAVLNRLLYAVGGFDGTNRLNSAECYPERNEWRMITAMNTIRSG
AGVCVLHNCIYAAGGYDGDQLNSVERYDVETETWTFVAPMKHRRSALGITVHQGRIYVLLGGYDGHFTLDSVECYDPD
TD TWSEVTRMTSGRSGVGVAVTMEPCRKQIDQQNCTC

Vector: pFB-LIC-Bse

Tag and additions: TEV-cleavable N-terminal hexahistidine tag

Expression cell: Sf9

KEAP1 BTB-BACK Kelch domains were cloned into the baculoviral transfer vector pFB-LIC-Bse. Bacmid was prepared from this vector in DH10Bac cells. Baculovirus was then prepared from this using Sf9 cells. Large scale baculoviral expression was performed for 72 hours at 27°C. The harvested cells were resuspended in 40 mL binding buffer (50 mM HEPES pH 7.5, 500 mM NaCl, 5 % glycerol, 5 mM imidazole and 0.5 mM TCEP) per 2L cell culture. PEI (1 mL) and protease inhibitors were added and the cells sonicated. After centrifugation of the lysate at 50 000 g the supernatant was filtered and incubated with 3 ml Ni²⁺ resin for 30 min. The column was washed with 50-80 ml wash buffer (50 mM HEPES pH 7.5, 500 mM NaCl, 5 % glycerol, 30 mM imidazole and 0.5 mM TCEP) and the protein eluted in 10 mL fractions of each of Elution buffers 1-4 (Binding buffer with increasing concentrations of imidazole – 50, 100, 150 and 250 mM). The fractions were pooled, diluted one third with binding buffer and TEV added for overnight incubation. The samples were concentrated, KEAP1 and Cul3 added together in a 1:1 molar ratio and incubated for 2 hours, before size exclusion purification on a 16/60 Superdex S200 column. Peak fractions were pooled, concentrated and stored at 4°C or -80°C.

Biotinylated KEAP1 BTB-3-box domains (used for assays)

Boundaries: residues 48-213

Expressed protein sequence:

MHHHHHHSSGVDLGTENLYFQSMGNRTFSYTLTDHTKQAFGIMNELRLSQQLCDVTLQVKYQDAPAAQFMAHKVVLASS
SPVFKAMFTNGLREQGMEVVSIEGIHPKVMERLIEFAYTASISMGEKCVLHVMMNGAVMYQIDSVVRACSDFLVQQLDPSNA
IGIANFAEQIGCVELHQRRAREYIYMHFGESSKGGYGLNDIFEAQKIEWHE

Vector: pNIC-Bio3

Tag and additions: TEV-cleavable N-terminal hexahistidine tag plus C-terminal avi tag for biotinylation

Expression cell: E. coli BL21(DE3)R3-pRARE2

Human KEAP1 BTB-3-box domains were cloned into the pNIC-Bio3 vector containing a His6 tag in the 22-aa N-terminal fusion peptide, with TEV protease cleavage site, and an avi tag sequence for biotinylation in the C-terminal fusion. The protein was co-expressed in *E.coli* containing a BirA vector for in cell biotinylation. Cells were grown at 37°C, 180 rpm for 2-3 hours in 2xYT medium containing 100 µM D-biotin until OD600 = 0.6 and were then induced with 0.4 mM IPTG and incubated with shaking at 18°C overnight. Biotin was prepared at 2.4 mg/mL (10 mM) in 10 mL of 10 mM Bicine, pH 8.3 and filter sterilised. A further 10 mL of this solution was added to the cell cultures the next morning for one hour before harvesting at 7000 g for 15 minutes at 4 °C. Protein was purified sequentially using Ni-affinity and size exclusion chromatography as for the KEAP1 BTB-3-box above.

Kelch selectivity panel proteins (used for crystallography and assays)

All Kelch domains were expressed from either a pNIC28-Bsa4 vector overnight at 18 °C in *E. coli* BL21(DE3)R3-pRARE2 cells (KEAP1, KLHL2, KLHL3, KLHL7, KLHL11, KLHL12, KLHL17, KLHL20, KBTBD5, KBTBD10, KLHDC4), with 0.4 mM IPTG induction, or utilising a pFB-LIC-Bse baculoviral transfer vector system in Sf9 baculoviral cultures (KLHL6, KLHL21, KBTBD7, KBTBD8, KLHDC5, KLHDC9) at 27°C for 72 hours in glass shaker flasks. Construct residue ranges are listed in **Fig. 9B**. All constructs were His-tagged and therefore purified using Nickel sepharose chromatography followed by TEV cleavage of the tag and gel filtration. Briefly, the harvested cells (2-3 L) were resuspended in 40 mL Binding Buffer (50 mM HEPES pH 7.5, 500 mM NaCl, 5 % glycerol, 5 mM imidazole and 0.5 mM TCEP) per 2 L cell culture. PEI (0.125%) and protease inhibitors were added and the cells sonicated. After centrifugation of the lysate at 50 000 g the supernatant was filtered (1.2 µm) and incubated rotating at 4 °C with 3 mL Ni²⁺ resin equilibrated in Binding Buffer, for 1 hour. The column was washed with 50-80 mL Wash Buffer (50 mM HEPES pH 7.5, 500 mM NaCl, 5 % glycerol, 30 mM imidazole and 0.5 mM TCEP) and the protein eluted in 5-10 mL fractions with each of Elution buffers 1-4 (Binding Buffer with increasing concentrations of imidazole: 50, 100, 150 and 250 mM). The fractions were pooled, diluted one third with binding buffer and tobacco etch virus (TEV) protease added for overnight incubation to remove the hexahistidine tag. The samples were concentrated in centrifugal concentrators (Sartorius Vivaspin 10 000 MWCO) before size exclusion purification on a 16/60 Superdex S200 column at 4°C in Gel Filtration (GF) Buffer (50 mM HEPES pH 7.5, 300 mM NaCl, 0.5 mM TCEP). Peak fractions were pooled and concentrated, subjected to a nickel rebind step if necessary, then snap frozen and stored at -80 °C.

Structure Determination

Human KEAP1 Kelch domain (PDB: [6ROG](#), 2.16 Å)

KEAP1 Kelch domain was crystallized using the vapour-diffusion technique in 150 nL sitting drops containing 50 nL protein (12 mg/mL) and 100 nL of a reservoir solution containing 4M sodium formate at 4 °C. Crystals were directly flash frozen in liquid nitrogen without addition of a cryo-protectant. Diffraction data were collected at 100K on Diamond Light Source beamline I04-1. Data were indexed and integrated using XDS (18) and scaled using AIMLESS (19) as part of the XIA2 auto-processing pipeline (20). The structure was solved by molecular replacement with PHASER (21) and PDB ID [1U6D](#) as a search model. Refinement was carried out with REFMAC5 (22) and manual rebuilding was performed with COOT (23). The refined structure was validated with MolProbity (24).

Human KEAP1 BTB-3-box and CUL3NTD complex (PDB: [5NLB](#), 3.45 Å)

Crystallisation was achieved at 20°C using the sitting drop vapour diffusion method. The protein complex crystallised in 150 nL drops at 9.4 mg/mL at a 1:2 ratio of protein to precipitant (20% PEG 3350, 10 % ethylene glycol, 0.2 M potassium citrate tribasic), using 20 nL of seeds previously prepared in a similar condition. Crystals were cryoprotected in 20 % ethylene glycol in well precipitant and then vitrified in liquid nitrogen. Diffraction data were collected at the Diamond Light Source, station I03 using monochromatic radiation at wavelength 0.97626 Å. Automated diffraction data reduction was performed using xia2 3d (20), and the indexed, integrated, scaled and merged data was phased using Phaser-MR in Phenix (25) with a structure of KLHL11 BTB-BACK complexed to CUL3 as the search model (PDB [4AP2](#)). The molecular replacement (MR) structure solution was refined using Phenix (25) and Buster (26) with manual rebuilding with Coot (23). Molprobity (24) was used to verify the geometrical correctness of the structure.

Assays

Biolayer interferometry

Biolayer interferometry (BLI) was used to determine the affinity of binding between KEAP1 BTB-3-box and CUL3NTD. Biotinylated KEAP1 (residues G48-E213) buffered in 50 mM HEPES, 300 mM NaCl, 0.5 mM TCEP, 10 mM DTT, was used at 0.16 mg/mL to immobilise 7-8 nm response units of protein to streptavidin-coated Octet sensors (ForteBio). Serial dilutions of CUL3 NTD (from 0.1563 to 5 µM) in the same buffer plus 0.01 % Tween were placed in the relevant wells, with buffer in the reference wells. Association and dissociation were set for 120 s each. Data were analysed using ForteBio Data Analysis 9.0 with local, partial fitting and double referencing.

Differential scanning fluorimetry

Differential scanning fluorimetry (DSF) was performed in triplicate using an Mx3005p real time PCR machine with 2 µM protein buffered in 10 mM HEPES pH 7.5, 150 mM NaCl, 0.5 mM TCEP, and 1:1000 dilution of Sypro orange. Compounds to be tested were added to a final concentration of 12.5 µM. 20 µL of each sample were placed in a 96-well plate and heated from 25 to 96°C. Fluorescence was monitored with excitation and emission filters set to 465 and 590 nm, respectively. Data were analysed with the MxPro software and curves fit in Microsoft Excel using the Boltzmann equation to determine the midpoint of thermal denaturation (T_m). Thermal shift values (ΔT_m) induced by inhibitor binding were calculated relative to control wells containing protein and 2.5% DMSO.

References

1. Petroski, M. D., and Deshaies, R. J. (2005) [Function and regulation of cullin-RING ubiquitin ligases](#). *Nature reviews. Molecular cell biology* **6**, 9-20
2. Duda, D. M., Borg, L. A., Scott, D. C., Hunt, H. W., Hammel, M., and Schulman, B. A. (2008) [Structural insights into NEDD8 activation of cullin-RING ligases: conformational control of conjugation](#). *Cell* **134**, 995-1006
3. Canning, P., Cooper, C. D., Krojer, T., Murray, J. W., Pike, A. C., Chaikuad, A., Keates, T., Thangaratnarajah, C., Hojzan, V., Marsden, B. D., Gileadi, O., Knapp, S., von Delft, F., and Bullock, A. N. (2013) [Structural basis for Cul3 protein assembly with the BTB-Kelch family of E3 ubiquitin ligases](#). *J Biol Chem* **288**, 7803-7814

4. Kobayashi, A., Kang, M. I., Okawa, H., Ohtsuji, M., Zenke, Y., Chiba, T., Igarashi, K., and Yamamoto, M. (2004) Oxidative stress sensor Keap1 functions as an adaptor for Cul3-based E3 ligase to regulate proteasomal degradation of Nrf2. *Mol Cell Biol* **24**, 7130-7139
5. Furukawa, M., and Xiong, Y. (2005) BTB protein Keap1 targets antioxidant transcription factor Nrf2 for ubiquitination by the Cullin 3-Roc1 ligase. *Mol Cell Biol* **25**, 162-171
6. Lo, S. C., Li, X., Henzl, M. T., Beamer, L. J., and Hannink, M. (2006) Structure of the Keap1:Nrf2 interface provides mechanistic insight into Nrf2 signaling. *EMBO J* **25**, 3605-3617
7. Fukutomi, T., Takagi, K., Mizushima, T., Ohuchi, N., and Yamamoto, M. (2014) Kinetic, thermodynamic, and structural characterizations of the association between Nrf2-DLGex degron and Keap1. *Mol Cell Biol* **34**, 832-846
8. McMahon, M., Itoh, K., Yamamoto, M., and Hayes, J. D. (2003) Keap1-dependent proteasomal degradation of transcription factor Nrf2 contributes to the negative regulation of antioxidant response element-driven gene expression. *J Biol Chem* **278**, 21592-21600
9. Padmanabhan, B., Tong, K. I., Ohta, T., Nakamura, Y., Scharlock, M., Ohtsuji, M., Kang, M. I., Kobayashi, A., Yokoyama, S., and Yamamoto, M. (2006) Structural basis for defects of Keap1 activity provoked by its point mutations in lung cancer. *Mol Cell* **21**, 689-700
10. Cuadrado, A., Rojo, A. I., Wells, G., Hayes, J. D., Cousin, S. P., Rumsey, W. L., Attucks, O. C., Franklin, S., Levonen, A. L., Kensler, T. W., and Dinkova-Kostova, A. T. (2019) Therapeutic targeting of the NRF2 and KEAP1 partnership in chronic diseases. *Nat Rev Drug Discov* **18**, 295-317
11. Davies, T. G., Wixted, W. E., Coyle, J. E., Griffiths-Jones, C., Hearn, K., McMenemy, R., Norton, D., Rich, S. J., Richardson, C., Saxty, G., Willems, H. M., Woolford, A. J., Cottom, J. E., Kou, J. P., Yonchuk, J. G., Feldser, H. G., Sanchez, Y., Foley, J. P., Bolognese, B. J., Logan, G., Podolin, P. L., Yan, H., Callahan, J. F., Heightman, T. D., and Kerns, J. K. (2016) Monoacidic Inhibitors of the Kelch-like ECH-Associated Protein 1: Nuclear Factor Erythroid 2-Related Factor 2 (KEAP1:NRF2) Protein-Protein Interaction with High Cell Potency Identified by Fragment-Based Discovery. *J Med Chem* **59**, 3991-4006
12. Heightman, T. D., Callahan, J. F., Chiarparin, E., Coyle, J. E., Griffiths-Jones, C., Lakdawala, A. S., McMenemy, R., Mortenson, P. N., Norton, D., Peakman, T. M., Rich, S. J., Richardson, C., Rumsey, W. L., Sanchez, Y., Saxty, G., Willems, H. M. G., Wolfe, L., 3rd, Woolford, A. J., Wu, Z., Yan, H., Kerns, J. K., and Davies, T. G. (2019) Structure-Activity and Structure-Conformation Relationships of Aryl Propionic Acid Inhibitors of the Kelch-like ECH-Associated Protein 1/Nuclear Factor Erythroid 2-Related Factor 2 (KEAP1/NRF2) Protein-Protein Interaction. *J Med Chem* **62**, 4683-4702
13. Canning, P., Sorrell, F. J., and Bullock, A. N. (2015) Structural basis of Keap1 interactions with Nrf2. *Free Radic Biol Med* **88**, 101-107
14. Errington, W. J., Khan, M. Q., Bueller, S. A., Rubinstein, J. L., Chakrabarty, A., and Prive, G. G. (2012) Adaptor protein self-assembly drives the control of a cullin-RING ubiquitin ligase. *Structure* **20**, 1141-1153
15. Canning, P., and Bullock, A. N. (2014) New strategies to inhibit KEAP1 and the Cul3-based E3 ubiquitin ligases. *Biochem Soc Trans* **42**, 103-107
16. Hu, L., Magesh, S., Chen, L., Wang, L., Lewis, T. A., Chen, Y., Khodier, C., Inoyama, D., Beamer, L. J., Emge, T. J., Shen, J., Kerrigan, J. E., Kong, A.-N. T., Dandapani, S., Palmer, M., Schreiber, S. L., and Munoz, B. (2013) Discovery of a small-molecule inhibitor and cellular probe of Keap1-Nrf2 protein-protein interaction. *Bioorganic & Medicinal Chemistry Letters* **23**, 3039-3043
17. Hur, W., Sun, Z., Jiang, T., Mason, D. E., Peters, E. C., Zhang, D. D., Luesch, H., Schultz, P. G., and Gray, N. S. (2010) A small-molecule inducer of the antioxidant response element. *Chem Biol* **17**, 537-547
18. Kabsch, W. (2010) Xds. *Acta Crystallogr D Biol Crystallogr* **66**, 125-132
19. Evans, P. R., and Murshudov, G. N. (2013) How good are my data and what is the resolution? *Acta Crystallogr D Biol Crystallogr* **69**, 1204-1214
20. Winter, G., Lobley, C. M., and Prince, S. M. (2013) Decision making in xia2. *Acta Crystallogr D Biol Crystallogr* **69**, 1260-1273
21. McCoy, A. J., Grosse-Kunstleve, R. W., Adams, P. D., Winn, M. D., Storoni, L. C., and Read, R. J. (2007) Phaser crystallographic software. *J Appl Crystallogr* **40**, 658-674

22. Murshudov, G. N., Skubak, P., Lebedev, A. A., Pannu, N. S., Steiner, R. A., Nicholls, R. A., Winn, M. D., Long, F., and Vagin, A. A. (2011) [REFMAC5 for the refinement of macromolecular crystal structures](#). *Acta Crystallogr D Biol Crystallogr* **67**, 355-367
23. Emsley, P., Lohkamp, B., Scott, W. G., and Cowtan, K. (2010) [Features and development of Coot](#). *Acta Crystallogr D Biol Crystallogr* **66**, 486-501
24. Chen, V. B., Arendall, W. B., 3rd, Headd, J. J., Keedy, D. A., Immormino, R. M., Kapral, G. J., Murray, L. W., Richardson, J. S., and Richardson, D. C. (2010) [MolProbity: all-atom structure validation for macromolecular crystallography](#). *Acta Crystallogr D Biol Crystallogr* **66**, 12-21
25. Adams, P. D., Afonine, P. V., Bunkoczi, G., Chen, V. B., Davis, I. W., Echols, N., Headd, J. J., Hung, L. W., Kapral, G. J., Grosse-Kunstleve, R. W., McCoy, A. J., Moriarty, N. W., Oeffner, R., Read, R. J., Richardson, D. C., Richardson, J. S., Terwilliger, T. C., and Zwart, P. H. (2010) [PHENIX: a comprehensive Python-based system for macromolecular structure solution](#). *Acta Crystallogr D Biol Crystallogr* **66**, 213-221
26. Bricogne, G., Blanc, E., Brandl, M., Flensburg, C., Keller, P., Paciorek, W., Roversi, P., Sharff, A., Smart, O. S., Vonrhein, C., Womack, T. O. (2016) [BUSTER version 2.10.2](#), in Cambridge, United Kingdom: Global Phasing Ltd.

We respectfully request that this document is cited using the DOI value as given above if the content is used in your work.